Journal of Computational Mathematics
Vol.30, No.4, 2012, 381–391.

http://www.global-sci.org/jcm
doi:10.4208/jcm.1111-m3679

TAILORED FINITE CELL METHOD FOR SOLVING HELMHOLTZ EQUATION IN LAYERED HETEROGENEOUS MEDIUM*

Zhongyi Huang
Department of Mathematical Sciences, Tsinghua University, Beijing 100084, China
Email: zhuang@math.tsinghua.edu.cn
Xu Yang
Department of Mathematics, Courant Institute of Mathematical Sciences, New York University, New York, NY 10012, USA
Email: xuyang@cims.nyu.edu

Abstract

In this paper, we propose a tailored finite cell method for the computation of two-dimensional Helmholtz equation in layered heterogeneous medium. The idea underlying the method is to construct a numerical scheme based on a local approximation of the solution to Helmholtz equation. This provides a computational tool of achieving high accuracy with coarse mesh even for large wave number (high frequency). The stability analysis and error estimates of this method are also proved. We present several numerical results to show its efficiency and accuracy.

Mathematics subject classification: 65N35, 35L10.
Key words: Tailored finite cell method, Helmholtz equation, Heterogeneous media, Sommerfeld condition.

1. Introduction

In this paper, we study the Helmholtz equation in a layered heterogeneous medium

$$\Delta u(\mathbf{x}) + k^2 n^2(x) u(\mathbf{x}) = f(\mathbf{x}), \qquad \text{for } \mathbf{x} = (x, y) \in \Omega, \tag{1.1}$$

$$u|_{x=0} = u_0(y), \quad \left(\frac{\partial u}{\partial x} - \mathrm{i} k n(x) u\right)\Big|_{x=R} = 0, \quad \text{for } y \in \mathbb{R}, \tag{1.2}$$

$$\frac{\partial u}{\partial r}(\mathbf{x}) - \mathrm{i} k n(x) u(\mathbf{x}) = o\left(\frac{1}{\sqrt{r}}\right), \quad \text{as} \quad r = |\mathbf{x}| \to +\infty, \tag{1.3}$$

where $\Omega = (0, R) \times \mathbb{R}$, $\mathrm{i} = \sqrt{-1}$ is the imaginary unit, k is the wave number, $f \in L^2(\Omega)$, $u_0 \in H^1(\mathbb{R})$. Here the index of refraction $n(x) \in L^\infty(0, R)$ is a piecewise smooth function, which satisfies

$$n_0 \leq n(x) \leq N_0. \tag{1.4}$$

The boundary value problem of the Helmholtz equation (1.1)–(1.3) arises in many physical fields, for example in seismic imaging where the interior structure of the Earth is layered indeed. Moreover, we can also see similar problems in acoustic wave propagation and electromagnetic wave propagation. The numerical computation of Helmholtz equation with large wave number

* Received February 10, 2011 / Revised version received October 11, 2011 / Accepted November 3, 2011 / Published online July 6, 2012 /

in heterogeneous medium is extremely difficult [2, 22–24] since the mesh size has to be small enough to resolve the wave length. In the last three decades, many scientists have presented efficient methods for this kind of problem, such as the fast multipole method [12], multifrontal method [27], discrete singular convolution method [4], hybrid numerical asymptotic method [11], spectral approximation method [32], element-free Galerkin method [36, 38], geometrical optics-based numerical method [6, 7], *etc.* In general one has the restriction $kh = \mathcal{O}(1)$ for the mesh size h to achieve a satisfactory numerical accuracy. On the other hand, if we use asymptotic method, we usually need to overcome the difficulties about caustics [6, 7, 10, 31].

Tailored finite point method (TFPM) was proposed by Han, Huang and Kellogg for the numerical solutions of singular perturbation problem [18] in 2008. TFPM is different from the typical finite point method [9, 26, 29, 30] which is a development of finite difference method by emphasizing the meshless technique. The main idea underlying the TFPM is to use the exact solution of the local approximate problem to construct the global approximation. Recently, TFPM has been further developed to solve various numerical problems. For example, Han and Huang studied TFPM for the Helmholtz equation in one dimension [13], and obtained the uniform convergence in L^2-norm with respect to the wave number. They also studied TFPM for different kinds of singular perturbation problems [14–16], without any prior knowledge of the boundary/interior layers. This method can provide high accuracy even on the uniform coarse mesh $h \gg \varepsilon$, where ε is the small parameter in the singular perturbation problem. For the interface problem [20], the method produces uniform convergence in energy norm even for the PDEs of mixed type. Later, Shih *et al* proposed a characteristic TFPM and rotated the stencil an angle to keep the grids be a streamline aligned [34,35], that improved the accuracy on coarse mesh. Furthermore, the method was applied to solve the steady MHD duct flow problems with boundary layers successfully [19]. TFPM also works well for time-dependent problem [21] and fourth-order singular perturbation problem [17]. More related work can be found in two review papers [5, 37] and the references therein. Note that there was also much work about meshless methods for Helmholtz equation [1, 3, 8, 28].

In this paper, we introduce a new approach to construct a discrete scheme for the equation (1.1) based on the former studies [13, 20]. We call the new scheme "*tailored finite cell method*" (TFCM), because it has been tailored to some local properties of the problem in each cell. As we consider the layered medium at here, we will apply our idea after a Fourier transform in y-direction. Hence this is a semi-discrete method designed on the properties of the local approximate problem. The method can achieve high accuracy with relatively cheap computational cost. Especially, we can get the exact solution with fixed points for piecewise linear coefficient for both small and large wave numbers.

2. Tailored Finite Cell Method

In this section, we describe the method in details. To be more precise, in the rest of this paper, we shall assume that the piecewise smooth function $n(x)$ is also piecewise monotone, *i.e.* there are some points χ_j $(j = 0, 1, \cdots, L)$ such that $0 = \chi_0 < \chi_1 < \cdots < \chi_L = R$, and

$$I_j = (\chi_{j-1}, \chi_j), \quad n|_{I_j} \in C^2(\bar{I}_j) \text{ and } n|_{I_j} \text{ is monotone}, \quad j = 1, \cdots, L.$$

First, we take a Fourier transform with respect to y, *i.e.* for $v(x, y) \in L^2(\Omega)$,

$$\hat{v}(x, \xi) \equiv \frac{1}{\sqrt{2\pi}} \int_{\mathbb{R}} v(x, y) e^{-\mathrm{i}\xi y} dy.$$

From (1.1)–(1.3), we have

$$\frac{\partial^2 \hat{u}}{\partial x^2}(x,\xi) + \left(k^2 n^2(x) - \xi^2\right) \hat{u}(x,\xi) = \hat{f}(x,\xi), \quad x \in (0,R),\ \xi \in \mathbb{R}, \tag{2.1a}$$

$$\hat{u}(0,\xi) = \hat{u}_0(\xi), \qquad \frac{\partial \hat{u}}{\partial x}(R,\xi) - \mathrm{i}kn(R)u(R,\xi) = 0, \quad \xi \in \mathbb{R}. \tag{2.1b}$$

We approximate the function $n^2(x)$ by a piecewise linear function $\widetilde{n}^2(x)$, *i.e.* we take a partition of the interval $(0,R)$ as $0 = x_0 < x_1 < \cdots < x_J = R$, such that
$\chi_l,\ l = 0,\cdots,L\} \subset \{x_j,\ j = 0,\cdots,J\}$ and

$$\widetilde{n}^2(x) = \alpha_j x + \beta_j, \quad \text{for } x \in (x_{j-1}, x_j), \qquad j = 1,\cdots,J, \tag{2.2a}$$

$$\alpha_j = \frac{n^2(x_j) - n^2(x_{j-1})}{x_j - x_{j-1}}, \quad \beta_j = n^2(x_{j-1}) - \alpha_j x_{j-1}, \qquad j = 1,\cdots,J. \tag{2.2b}$$

Denote by $h = \max\limits_{1\le j\le J} |x_j - x_{j-1}|$, we have

$$|\widetilde{n}^2(x) - n^2(x)| \le Ch^2, \quad \text{for } x \in [0,R]. \tag{2.3}$$

For $j = 1,\cdots,J$, let $a_j = k^2\alpha_j$, $\quad b_j = k^2\beta_j - \xi^2$, we have three cases:
I). If $a_j = b_j = 0$, let

$$G_j(x,s) = \begin{cases} s - x, & x \ge s, \\ 0, & s \ge x. \end{cases} \tag{2.4}$$

Then the solution of (2.1a) in D_j can be expressed by

$$U_h(x,\xi) = A_j(\xi) + B_j(\xi)x + \int_{x_{j-1}}^{x_j} \hat{f}(s,\xi) G_j(x,s) ds, \quad \text{for } x \in D_j. \tag{2.5}$$

Let

$$\lambda_j^+ = \lambda_j^- = 1, \quad \gamma_j^+ = \gamma_j^- = 0, \quad \mu_j^+ = x_j, \quad \mu_j^- = x_{j-1}, \quad \delta_j^+ = \delta_j^- = 1,$$

$$F_j^+(\xi) = \int_{x_{j-1}}^{x_j} \hat{f}(s,\xi)(s - x_j) ds, \quad F_j^- = 0, \tag{2.6}$$

$$G_j^+(\xi) = -\int_{x_{j-1}}^{x_j} \hat{f}(s,\xi) ds,\ G_j^- = 0. \tag{2.7}$$

II). If $a_j = 0$, $b_j \ne 0$, let

$$G_j(x,s) = \frac{1}{2\sqrt{b_j}} \begin{cases} \sinh\sqrt{b_j}(s - x), & x \ge s, \\ \sinh\sqrt{b_j}(x - s), & s \ge x. \end{cases} \tag{2.8}$$

Then the solution of (2.1a) in D_j can be expressed by

$$U_h(x,\xi) = A_j(\xi) e^{x\sqrt{b_j}} + B_j(\xi) e^{-x\sqrt{b_j}} + \int_{x_{j-1}}^{x_j} \hat{f}(s,\xi) G_j(x,s) ds, \quad \text{for } x \in D_j, \tag{2.9}$$

Let

$$\lambda_j^+ = \mathrm{e}^{x_j\sqrt{b_j}}, \quad \lambda_j^- = \mathrm{e}^{x_{j-1}\sqrt{b_j}}, \quad \gamma_j^+ = \sqrt{b_j}\,\mathrm{e}^{x_j\sqrt{b_j}}, \quad \gamma_j^- = \sqrt{b_j}\,\mathrm{e}^{x_{j-1}\sqrt{b_j}},$$

$$\mu_j^+ = \mathrm{e}^{-x_j\sqrt{b_j}}, \quad \mu_j^- = \mathrm{e}^{-x_{j-1}\sqrt{b_j}},$$

$$\delta_j^+ = -\sqrt{b_j}\,\mathrm{e}^{-x_j\sqrt{b_j}}, \quad \delta_j^- = -\sqrt{b_j}\,\mathrm{e}^{-x_{j-1}\sqrt{b_j}},$$

$$F_j^+(\xi)=\int_{x_{j-1}}^{x_j}\hat f(s,\xi)G_j(x_j,s)ds,\quad G_j^+(\xi)=\int_{x_{j-1}}^{x_j}\hat f(s,\xi)\partial_x G_j(x,s)\big|_{x=x_j}ds, \tag{2.10}$$

$$F_j^-(\xi)=\int_{x_{j-1}}^{x_j}\hat f(s,\xi)G_j(x_{j-1},s)ds,\quad G_j^-(\xi)=\int_{x_{j-1}}^{x_j}\hat f(s,\xi)\partial_x G_j(x,s)\big|_{x=x_{j-1}}ds. \tag{2.11}$$

III). If $a_j\neq 0$, let

$$z(x)=-(a_j)^{-\frac{2}{3}}(a_jx+b_j),\quad z_{j-1}=z(x_{j-1}),\quad z_j=z(x_j),$$

$$\widetilde{f}(s,\xi)=(a_j)^{-\frac{2}{3}}\hat f\left((a_j)^{-\frac{1}{3}}s-\frac{b_j}{a_j},\xi\right),$$

$$G_j(t,s)=-\frac{1}{2}\begin{cases}\mathrm{Ai}(s)\mathrm{AI}(t)+\mathrm{Bi}(s)\mathrm{BI}(t), t\geq s,\\ \mathrm{Ai}(s)\mathrm{AI}(s)+\mathrm{Bi}(s)\mathrm{BI}(s), s\geq t,\end{cases} \tag{2.12}$$

where $\mathrm{Ai}(s)$ and $\mathrm{Bi}(s)$ are the Airy functions of the first and second kind respectively, and

$$\mathrm{AI}(t)=\int_0^t\big(\mathrm{Ai}(\eta)\big)^{-2}d\eta,\quad \mathrm{BI}(t)=\int_0^t\big(\mathrm{Bi}(\eta)\big)^{-2}d\eta.$$

Then the solution of (2.1a) in D_j can be expressed by

$$U_h\big(z(x),\xi\big)=A_j(\xi)\mathrm{Ai}\big(z(x)\big)+B_j(\xi)\mathrm{Bi}\big(z(x)\big)+\int_{z_{j-1}}^{z_j}\widetilde{f}(x,\xi)(s)G_j\big(z(x),s\big)ds,\ \forall x\in D_j,$$

with two constants $A_j,B_j\in\mathbb{R}$. Let

$$\begin{aligned}
&\lambda_j^+=\mathrm{Ai}\big(z(x_j)\big), && \lambda_j^-=\mathrm{Ai}\big(z(x_{j-1})\big), && \gamma_j^+=(a_j)^{\frac{1}{3}}\mathrm{Ai}'\big(z(x_j)\big),\\
&\gamma_j^-=(a_j)^{\frac{1}{3}}\mathrm{Ai}'\big(z(x_{j-1})\big), && \mu_j^+=\mathrm{Bi}\big(z(x_j)\big), && \mu_j^-=\mathrm{Bi}\big(z(x_{j-1})\big),\\
&\delta_j^+=(a_j)^{\frac{1}{3}}\mathrm{Bi}'\big(z(x_j)\big), && \delta_j^-=(a_j)^{\frac{1}{3}}\mathrm{Bi}'\big(z(x_{j-1})\big), &&
\end{aligned}$$

$$F_j^+(\xi)=\int_{z_{j-1}}^{z_j}\widetilde{f}(s,\xi)G_j\big(z(x_j),s\big)ds, \tag{2.13a}$$

$$G_j^+(\xi)=\int_{z_{j-1}}^{z_j}\widetilde{f}(s,\xi)\partial_x G_j\big(z(x),s\big)\big|_{x=x_j}ds, \tag{2.13b}$$

$$F_j^-(\xi)=\int_{z_{j-1}}^{z_j}\widetilde{f}(s,\xi)G_j\big(z(x_{j-1}),s\big)ds, \tag{2.14a}$$

$$G_j^-(\xi)=\int_{z_{j-1}}^{z_j}\widetilde{f}(s,\xi)\partial_x G_j\big(z(x),s\big)\big|_{x=x_{j-1}}ds. \tag{2.14b}$$

From (2.4)–(2.14b), considering the boundary conditions (2.1b) and the continuities of $\hat u(x,\xi)$ at x_j $(j=1,\cdots,J-1)$, we have

$$\lambda_1^-A_1+\mu_1^-B_1+F_1^-=\hat u_0, \tag{2.15a}$$

$$\gamma_J^+A_J+\delta_J^+B_J+G_J^+-\mathrm{i}kn(R)\left(\lambda_J^+A_J+\mu_J^+B_J+F_J^+\right)=0, \tag{2.15b}$$

and for $1\leq j\leq J-1$,

$$\begin{cases}\lambda_j^+A_j+\mu_j^+B_j+F_j^+=\lambda_{j+1}^-A_{j+1}+\mu_{j+1}^-B_{j+1}+F_{j+1}^-,\\ \gamma_j^+A_j+\delta_j^+B_j+G_j^+=\gamma_{j+1}^-A_{j+1}+\delta_{j+1}^-B_{j+1}+G_{j+1}^-.\end{cases} \tag{2.16}$$

Solving the linear system (2.15)–(2.16) gives the coefficients $A_j(\xi)$ and $B_j(\xi)$, $j=1,\cdots,J$.

Finally, we obtain the solution of (1.1)–(1.3) by the inverse Fourier transform

$$u_h(x,y)=\frac{1}{\sqrt{2\pi}}\int_{\mathbb{R}}U_h\big(z(x),\xi\big)e^{\mathrm{i}\xi y}d\xi. \tag{2.17}$$

3. Stability Analysis

In this section, we study the stability estimate of the model problem (1.1)–(1.3) and the error analysis of our discrete solution by (2.17). First, we establish the following regularity estimate.

Lemma 3.1 (regularity estimate for analytic solution) *Suppose that* $n(x) \in L^\infty(0,R)$ *is piecewise smooth and piecewise monotone,* $f \in L^2(\Omega)$. *Then the solution of the problem* (1.1)–(1.3), $u(x,y)$, *satisfies the following estimates*

$$|u|_{1,\Omega} + k\|u\|_{0,\Omega} \le C\bigg(\|f\|_{L^2(\Omega)} + k\|u_0\|_{L^2(\mathbb{R})} + \|u_0'\|_{L^2(\mathbb{R})}\bigg), \tag{3.1}$$

with a constant C *independent of the wave number* k.

Proof. Let $U(x,y) = u(x,y) + u_0(y)(Ax-1)$ with $A = \frac{\mathrm{i}kn(R)}{\mathrm{i}kn(R)R-1}$. Then we have

$$\Delta U(x,y) + k^2 n^2(x) U(x,y) = F(x,y), \qquad (x,y) \in \Omega, \tag{3.2}$$

$$U(0,y) = 0, \quad U_x(R,y) - \mathrm{i}kn(R)U(R,y) = 0, \quad y \in \mathbb{R}, \tag{3.3}$$

$$U_r(x,y) - \mathrm{i}kn(x)U(x,y) = o\left(\frac{1}{\sqrt{r}}\right), \quad \text{as } r = \sqrt{x^2+y^2} \to \infty, \tag{3.4}$$

with

$$F(x,y) = f(x,y) + k^2 n^2(x)(Ax-1)u_0(y) + (Ax-1)u_0''(y).$$

From the boundary conditions (3.3), we can immediately get

$$\|U\|_{L^2(\Omega)} \le R\|U_x\|_{L^2(\Omega)}. \tag{3.5}$$

Multiplying (3.2) by $\bar{U}$ and integrating over Ω yields

$$\mathrm{i}kn(R)\int_{\mathbb{R}} |U(R,y)|^2 dy - \int_{\mathbb{R}}\int_0^R \left(|\nabla U|^2 - k^2 n^2(x)|U|^2\right) dxdy = \int_{\mathbb{R}}\int_0^R F\bar{U} dxdy.$$

Taking the real and imaginary parts of the above equation gives

$$\begin{aligned}
&-\int_{\mathbb{R}}\int_0^R \left(|\nabla U|^2 - k^2 n^2(x)|U|^2\right) dxdy = \mathrm{Re}\int_{\mathbb{R}}\int_0^R F\bar{U} dxdy,\\
&kn(R)\int_{\mathbb{R}} |U(R,y)|^2 dy = \mathrm{Im}\int_{\mathbb{R}}\int_0^R F\bar{U}\, dxdy.
\end{aligned}$$

Using Cauchy's inequality and the expression of function F produces, $\forall \varepsilon_j > 0, j = 1,\cdots,6$,

$$\begin{aligned}
&\Big|k^2\|nU\|^2_{L^2(\Omega)} - \|\nabla U\|^2_{L^2(\Omega)}\Big| \le \frac{\varepsilon_1}{2}\|U\|^2_{L^2(\Omega)} + \frac{1}{2\varepsilon_1}\|f\|^2_{L^2(\Omega)}\\
&\quad + k^2\left(\frac{1}{2\varepsilon_2}\|nu_0\|^2_{L^2(\Omega)} + \frac{\varepsilon_2}{2}\|nU\|^2_{L^2(\Omega)}\right) + \frac{1}{2\varepsilon_3}\|u_0'\|^2_{L^2(\Omega)} + \frac{\varepsilon_3}{2}\|U_y\|^2_{L^2(\Omega)},
\end{aligned} \tag{3.6}$$

$$\begin{aligned}
&kn(R)\|U(R,\cdot)\|^2_{L^2(\mathbb{R})} \le \frac{\varepsilon_4}{2}\|U\|^2_{L^2(\Omega)} + \frac{\|f\|^2_{L^2(\Omega)}}{2\varepsilon_4}\\
&\quad + k^2\left(\frac{1}{2\varepsilon_5}\|nu_0\|^2_{L^2(\Omega)} + \frac{\varepsilon_5}{2}\|nU\|^2_{L^2(\Omega)}\right) + \frac{1}{2\varepsilon_6}\|u_0'\|^2_{L^2(\Omega)} + \frac{\varepsilon_6}{2}\|U_y\|^2_{L^2(\Omega)}.
\end{aligned} \tag{3.7}$$

It is similar to the procedure of Lemma 2.1 in [13], we can define a function $z(x)$, such that

$$z(0)=0,\quad 0\le z(x)\le C,\quad 1\le z'(x)\le C, \tag{3.8a}$$
$$n_0^2\le \left(z(x)n^2(x)\right)',\quad \text{for}\ \ x\in[0,R]. \tag{3.8b}$$

Multiplying (3.2) by $\left(z(x)\bar{U}_x+z'(x)y\bar{U}_y\right)$ and integrating over Ω and taking the real part yield

$$\begin{aligned}&k^2n^2(R)z(R)\|U(R,\cdot)\|^2_{L^2(\mathbb{R})}-\int_{\mathbb{R}}\int_0^R k^2\left((zn^2)'+z'n^2\right)|U|^2dxdy-\int_0^R\frac{z^2(R)}{2}|U_y(R,y)|^2dy\\ &=\mathrm{Re}\int_{\mathbb{R}}\int_0^R F(x,y)\left(z(x)\bar{U}_x(x,y)+z'(x)y\bar{U}_y(x,y)\right)dxdy.\end{aligned}$$

Using Cauchy's inequality and the properties (1.4), (3.8), we have, $\forall\varepsilon_7,\varepsilon_8,\varepsilon_9>0$,

$$\begin{aligned}2k^2n_0^2\|U\|^2_{L^2(\Omega)}\le &C\left(k^2\|U(R,\cdot)\|^2_{L^2(\mathbb{R})}+\frac{k^2}{2\varepsilon_7}\|u_0\|^2_{L^2(\mathbb{R})}+\frac{\varepsilon_7k^2}{2}\|U\|^2_{L^2(\Omega)}\right)\\ &+\frac{\varepsilon_8}{2}\|\nabla U\|^2_{L^2(\Omega)}+\frac{1}{2\varepsilon_8}\|u_0'\|^2_{L^2(\mathbb{R})}+\frac{\varepsilon_9}{2}\|\nabla U\|^2_{L^2(\Omega)}+\frac{1}{2\varepsilon_9}\|f\|^2_{L^2(\Omega)}.\end{aligned} \tag{3.9}$$

Combining with (3.6)–(3.7) and choosing ε_j small enough, we get

$$\|\nabla U\|^2_{L^2(\Omega)}+k^2\|U\|^2_{L^2(\Omega)}\le C\left(\|f\|^2_{L^2(\Omega)}+k^2\|u_0\|^2_{L^2(\mathbb{R})}+\|u_0'\|^2_{L^2(\mathbb{R})}\right).$$

That implies (3.1) immediately. □

Suppose that $u(x,y)$ is the solution of problem (1.1)–(1.3), $u_h(x,y)$ is the approximation obtained by our method in Section 2 from (2.17). Let $E(x,y)=u(x,y)-u_h(x,y)$, be the error of our approximation. Then $E(x,y)$ satisfies the following problem

$$\Delta E(x,y)+k^2\widetilde{n}^2(x)E(x,y)=k^2\left(\widetilde{n}^2(x)-n^2(x)\right)u(x,y),\quad (x,y)\in\Omega, \tag{3.10}$$
$$E(0,y)=0,\qquad E_x(R,y)+\mathrm{i}kn(R)E(R,y)=0, \tag{3.11}$$
$$E_r(x,y)-\mathrm{i}kn(x)E(x,y)=o\left(\frac{1}{\sqrt{r}}\right),\quad \text{as}\ r=\sqrt{x^2+y^2}\to\infty, \tag{3.12}$$

By Lemmas 3.1 and Eq. (2.3), we arrive at the following result immediately.

Theorem 3.1 (error estimates) *Suppose that $n(x)\in L^\infty(0,R)$ is piecewise smooth and piecewise monotone, $f\in L^2(\Omega)$. Then the error function E satisfies the following estimate:*

$$|E|_{1,\Omega}+k\|E\|_{0,\Omega}\le Ckh^2\left(\|f\|_{L^2(\Omega)}+k\|u_0\|_{L^2(\mathbb{R})}+|u_0|_{H^1(\mathbb{R})}\right), \tag{3.13}$$

with a constant C independent of the wave number k and mesh size h.

4. Numerical Examples

In this section, we present some numerical examples to show the efficiency and reliability of our new method.

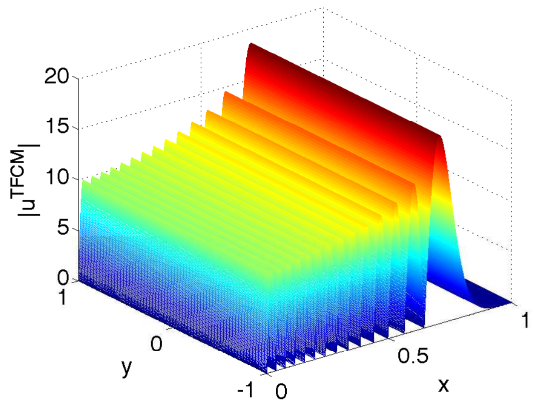

Fig. 4.1. Example 4.1 with $k = 100$, $h = \frac{1}{4}$, $n(x) = 1 - x$.

Example 4.1. First, for a sake of simplicity, we consider

$$\Delta u(\mathbf{x}) + k^2 n^2(x) u(\mathbf{x}) = f(\mathbf{x}), \qquad \text{for } \mathbf{x} = (x, y) \in \Omega = (0, R) \times (-L, L), \tag{4.1}$$

$$u|_{x=0} = u_0(y), \quad \left(\frac{\partial u}{\partial x} - \mathrm{i}kn(x)u\right)\Big|_{x=R} = 0, \quad \text{for } y \in (-L, L), \tag{4.2}$$

with a periodic boundary condition in y-direction, and

$$f(x) \equiv 0, \qquad n^2(x) = 1 - x, \qquad u_0(y) = e^{iky/2}, \quad R = L = 1.$$

The exact solution is

$$u(x, y) = e^{iky/2} \frac{\mathrm{Ai}\left(k^{2/3}(x - \frac{3}{4})\right)}{\mathrm{Ai}\left(-\frac{3}{4}k^{2/3}\right)}.$$

Note that there is a caustic line at $x = 0.75$ if we use WKB asymptotic expansion to solve this problem (*cf.* [6,7]). But there is no caustic by our method (*cf.* Fig. 4.1). We give the error of u^{TFCM} (the approximation by our TFCM) in Fig. 4.2 (a). Because $n^2(x)$ is a linear function, from Fig. 4.2 (a), we can see that our method can achieve the machine accuracy in this case, although our mesh size h is much larger than the wavelength.

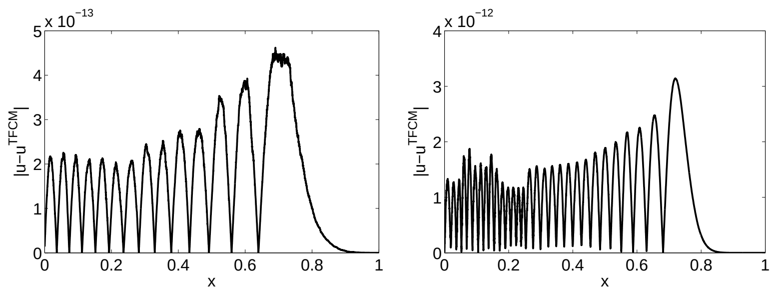

(a) (b)

Fig. 4.2. Errors of Example 4.1 at $y = 0$ with $k = 100$, $h = \frac{1}{4}$. (a): $n(x) = 1 - x$, (b): $n(x)$ given by (4.3).

Table 4.1: Example 4.2, the ℓ^∞ and relative ℓ^2 errors for TFCM, $k = 500$.

h	2^{-5}	2^{-6}	2^{-7}	2^{-8}
ℓ^∞ error	1.35×10^{-1}	3.71×10^{-2}	9.49×10^{-3}	2.38×10^{-3}
ℓ^2 error	6.83×10^{-2}	1.84×10^{-2}	4.76×10^{-3}	1.19×10^{-3}

Table 4.2: Example 4.3, the ℓ^∞ and relative ℓ^2 errors for TFCM, $k = 400$.

h	2^{-5}	2^{-6}	2^{-7}	2^{-8}
ℓ^∞ error	4.96×10^{-1}	1.36×10^{-1}	3.44×10^{-2}	8.84×10^{-3}
ℓ^2 error	1.71×10^{-1}	4.72×10^{-2}	1.21×10^{-2}	3.08×10^{-3}

Furthermore, even if $n^2(x)$ is a piecewise linear function, for example,

$$n^2(x) = \begin{cases} 1 + x, & x \in [0, 0.25); \\ 1 - x, & x \in [0.25, 1]; \end{cases} \tag{4.3}$$

we can also achieve the machine accuracy (*cf.* Fig. 4.2 (b)) with only one node in each subdomain.

Example 4.2. Then we consider a more complex case with $n^2(x) = 0.6 + 0.5x - x^2$.

In this case, the 'exact' solution is solved on very fine mesh $h = \frac{1}{8192}$. The results of this example are given in Fig. 4.3 and Table 4.1. Because $n^2(x)$ is not a linear function anymore, we can not achieve the machine accuracy in this case. But we still have the second order convergence rate from Table 4.1, although our mesh size h is much larger than the wavelength. It is consistent with our theoretical result (*cf.* Theorem 3.1).

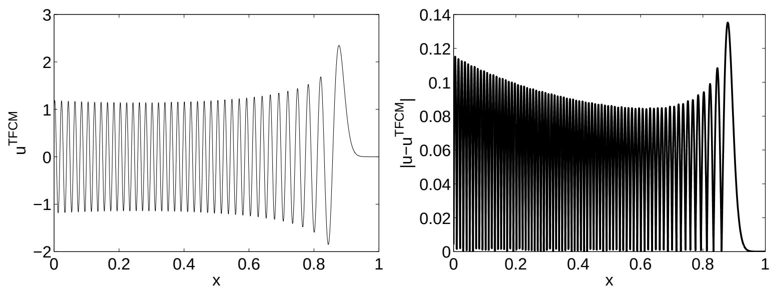

Fig. 4.3. The approximation and the error of Example 4.2 at $y = 0$: $k = 500$, $h = \frac{1}{32}$.

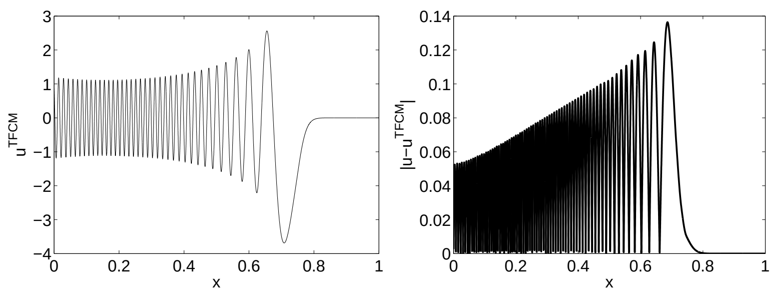

Fig. 4.4. The approximation and the error of Example 4.3 at $y = 0$: $k = 400$, $h = \frac{1}{64}$.

Example 4.3. Next we consider a case with discontinuous index of refraction

$$n^2(x) = \begin{cases} e^{-2x}\left(1+\sin(2\pi x)\right)+0.25, & x \in [0, 0.75]; \\ 1-x, & x \in (0.75, 1]. \end{cases}$$

Here the 'exact' solution is also solved on very fine mesh $h = \frac{1}{8192}$. The results of this example are given in Fig. 4.4 and Table 4.2. We still have the second order convergence rate from Table 4.2.

Example 4.4. Finally we consider a more complex case with discontinuous index of refraction

$$n^2(x) = \begin{cases} \cos(\pi x) - 0.5, & x \in [0, 0.25); \\ 1+x, & x \in [0.25, 0.5); \\ 1-x^2, & x \in [0.5, 0.75); \\ 1-x, & x \in [0.75, 1]. \end{cases}$$

In this case, the 'exact' solution is also solved on very fine mesh $h = \frac{1}{8192}$. The results of this example are given in Fig. 4.5 and Table 4.3. The convergence rate is also of second order.

Table 4.3: Example 4.4, the ℓ^∞ and relative ℓ^2 errors for TFCM, $k = 200$.

h	2^{-5}	2^{-6}	2^{-7}	2^{-8}
ℓ^∞ error	2.37×10^{-1}	6.09×10^{-2}	1.54×10^{-2}	3.88×10^{-3}
ℓ^2 error	7.14×10^{-2}	1.75×10^{-2}	4.47×10^{-3}	1.12×10^{-3}

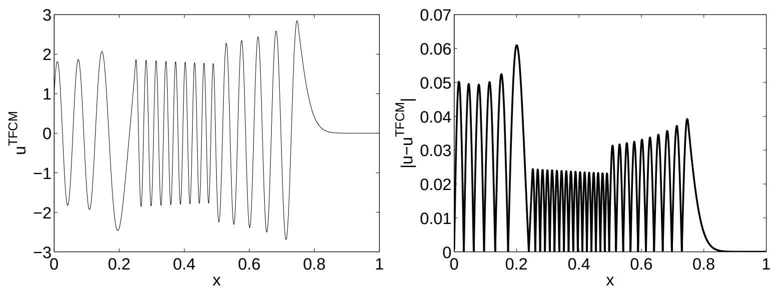

Fig. 4.5. The approximation and the error of Example 4.4 at $y = 0$, $k = 200$, $h = \frac{1}{64}$.

5. Conclusion

In this paper, we present a tailored finite cell method for Helmholtz equation in the layered heterogenous medium. This is a semi-discrete method designed on the properties of the local approximate problem. Following the idea of our previous works about TFPM [13,20], we solve the problem numerically after taking the Fourier transform in y-direction and approximating the squared index of refraction function using piecewise linear function. We analyze the stability of the original problem, prove the second order convergence rate of the method, and present several numerical examples to confirm the theoretical results. The numerical examples also show that this method can achieve high accuracy on coarse mesh even with discontinuous coefficient.

When the coefficient $n^2(\mathbf{x})$ is a piecewise linear function, we can obtain the exact solution with only one point in each subdomain. The method applied to more general cases will be studied later.

Acknowledgments. This work was supported by the NSFC Project No. 11071139, the National Basic Research Program of China under the grant 2011CB309705, Tsinghua University Initiative Scientific Research Program.

References

[1] C.J.S. Alves and C.S. Chen, A new method of fundamental solutions applied to nonhomogeneous elliptic problems, *Adv. Comput. Math.*, **23** (2005), 125-142.

[2] I.M. Babuška and S.A. Sauter, Is the pollution effect of the FEM avoidable for the Helmholtz equation considering high wave numbers?, *SIAM Rev.*, **42** (2000), 451-484.

[3] I. Babuška and J.M. Melenk, The partition of unity method, *Int. J. Numer. Meth. Engng.,* **40** (1997), 727-758.

[4] G. Bao, G.W. Wei and S. Zhao, Numerical solution of the Helmholtz equation with high wavenumbers, *Int. J. Numer. Meth. Engng.,* **59** (2004), 389-408.

[5] T. Belytschko, Y. Krongauz, D. Organ, M. Fleming and P. Krysl, Meshless methods: An overview and recent developments, *Comput. Method. Appl. M.,* **139** (1996), 3-47.

[6] J.D. Benamoua, O.Lafitte, R. Sentis and I. Solliec, A geometrical optics-based numerical method for high frequency electromagnetic fields computations near fold caustics — Part I, *J. Comput. Appl. Math.,* **156** (2003), 93-125.

[7] J.D. Benamoua, O.Lafitte, R. Sentis and I. Solliec, A geometric optics method for high-frequency electromagnetic fields computations near fold caustics — Part II. The energy, *J. Comput. Appl. Math.,* **167** (2004), 91-134.

[8] P. Bouillarda and S. Suleaub, Element-Free Galerkin solutions for Helmholtz problems: fomulation and numerical assessment of the pollution effect, *Comput. Method. Appl. M.,* **162** (1998), 317-335.

[9] M. Cheng and G.R. Liu, A novel finite point method for flow simulation, *Int. J. Numer. Meth. Fluids,* **39** (2002), 1161-1178.

[10] V. Cerveny, M.M. Popov and I. Psencik, Computation of wave fields in inhomogeneous media – Gaussian beam approach, *Geophys. J. Roy. Astr. Soc.,* **70** (1982), 109-128.

[11] E. Giladi and J.B. Keller, A hybrid numerical asymptotic method for scattering problems, *J. Comput. Phys.,* **174** (2001), 226-247.

[12] N. Gumerov and R. Duraiswami, Fast Multipole Methods for the Helmhotlz Equation in Three Dimensions, Elsevier, Oxford, 2005.

[13] H. Han and Z. Huang, A tailored finite point method for the Helmholtz equation with high wave numbers in heterogeneous medium, *J. Comput. Math.,* **26** (2008), 728-739.

[14] H. Han and Z. Huang, Tailored finite point method for a singular perturbation problem with variable coefficients in two dimensions, *J. Sci. Comput.,* **41** (2009), 200-220.

[15] H. Han and Z. Huang, Tailored finite point method for steady-state reaction-diffusion equation, *Commun. Math. Sci.,* **8** (2010), 887-899.

[16] H. Han and Z. Huang, Tailored finite point method based on exponential bases for convection-diffusion-reaction equation, *Math. Comput.,* (in press).

[17] H. Han and Z. Huang, An equation decomposition method for the numerical solution of a fourth-order elliptic singular perturbation problem, *Numer. Meth. Part. D. E.,* **28** (2012), 942-953.

[18] H. Han, Z. Huang and B. Kellogg, A Tailored finite point method for a singular perturbation problem on an unbounded domain, *J. Sci. Comput.,* **36** (2008), 243-261.

[19] P. Hsieh, Y. Shih and S. Yang, A tailored finite point method for solving steady MHD duct flow problems with boundary layers, *Commun. Comput. Phys.,* **10** (2011), 161-182.

[20] Z. Huang, Tailored finite point method for the interface problem, *Netw. Heterog. Media,* **4** (2009), 91-106.

[21] Z. Huang and X. Yang, Tailored finite point methods for first order wave equation, *J Sci. Comput.,* **49** (2011), 351-366.

[22] F. Ihlenburg and I. Babuška, Finite element solution of the Helmholtz equation with high wavenumber part I: the h-version of the FEM, *Comput. Math. Appl.,* **30** (1995), 9-37.

[23] F. Ihlenburg and I. Babuška, Finite element solution of the Helmholtz equation with high wavenumber part II: the h-p-version of the FEM, *SIAM J. Numer. Anal.,* **34** (1997), 315-358.

[24] S. Kim, C.S. Shin and J.B. Keller, High-frequency asymptotics for the numerical solution of the Helmholtz equation, *Appl. math. lett.,* **18** (2005), 797-804.

[25] S.-Y. Leung and H.-K. Zhao, Gaussian beam summation for diffraction in inhomogeneous media based on the grid based particle method. *Commun. Comput. Phys.,* **8** (2010), 758-796.

[26] H. Lin, S.N. Atluri, The meshless local Petrov-Galerkin (MLPG) method for solving incompressible Navier-Stokes equations, *CMES,* **2** (2001), 117-142.

[27] J. Liu, The multifrontal method for sparse matrix solution: theory and practice, *SIAM Rev.,* **34** (1992), 82-109.

[28] L. Marin, A meshless method for the numerical solution of the Cauchy problem associated with three-dimensional Helmholtz-type equations, *Appl. Math. Comput.,* **165** (2005), 355-374.

[29] B. Mendez and A. Velazquez, Finite point solver for the simulation of 2-D laminar incompressible unsteady flows, *Comput. Method. Appl. M.,* **193** (2004), 825-848.

[30] E. Oñate, S. Idelsohn, O.C. Zienkiewicz and R.L. Taylor, A finite point method in computational mechanics. Applications to convective transport and fluid flow, *Int. J. Numer. Meth. Eng.,* **39** (1996), 3839-3866.

[31] M.M. Popov, Taylor expansion and discretization errors in Gaussian beam superposition, *Wave Motion,* **4** (1982), 85-97.

[32] J. Shen and L.L. Wang, Spectral approximation of the Helmholtz equation with high wave numbers, *Siam J. Numer. Anal.,* **43** (2005), 623-644.

[33] Q. Sheng and H.-W. Sun, Asymptotic stability of an eikonal transformation based ADI method for the paraxial Helmholtz equation at high wave numbers. *Commun. Comput. Phys.,* **12** (2012), 1275-1292.

[34] Y. Shih, B. Kellogg and P. Tsai, A tailored finite point method for convection-diffusion-reaction problems, *J. Sci. Comput.,* **43** (2010), 239-260.

[35] Y. Shih, B. Kellogg and Y. Chang, Characteristics tailored finite point method for convection-dominated convection-diffusion-reaction problems, *J. Sci. Comput.,* **47** (2011), 198-215.

[36] S. Suleau and P. Bouillard, One-dimensional dispersion analysis for the element-free Galerkin method for the Helmholtz equation, *Int. J. Numer. Meth. Eng.,* **47** (2000), 1169-1188.

[37] L.L. Thompson, A review of finite-element methods for time-harmonic acoustics, *J. Acoust. Soc. Am.,* **119** (2006), 1315-1330.

[38] L.L. Thompson and P.M. Pinsky, A Galerkin least squares finite element method for the two-dimensional Helmholtz equation, *Int. J. Numer. Meth. Eng.,* **38** (1995), 371-397.